Available online at www.sciencedirect.com

SciVerse ScienceDirect

Scripta Materialia 65 (2011) 982–985

Scripta MATERIALIA

www.elsevier.com/locate/scriptamat

Bonding of immiscible Mg and Fe via a nanoscale Fe_2Al_5 transition layer

L. Liu,[a,b,*] L. Xiao,[b] J. Feng,[a] L. Li,[a] S. Esmaeili[b] and Y. Zhou[b]

[a] *State Key Laboratory of Advanced Welding Production Technology, Harbin Institute of Technology, Harbin 150001, People's Republic of China*

[b] *Department of Mechanical and Mechatronics Engineering, University of Waterloo, Waterloo, Canada N2L 3G1*

Received 1 August 2011; revised 27 August 2011; accepted 28 August 2011
Available online 31 August 2011

Bonding of immiscible systems is difficult due to the sharp interface and high interfacial energy. A nanoscale transition layer with lattice matching to both sides could be a solution. To examine this hypothesis, Mg and Fe were successfully bonded by a precoated nanoscale Fe_2Al_5 layer, which in crystallographic terms matched well with both lattices. The interplanar mismatches of both Fe_2Al_5/Fe and Fe_2Al_5/Mg interfaces were less than 5% and both interfaces were found to be semicoherent.

Keywords: Bonding; Orientation relationships; Immiscible system; Intermetallic compounds; Magnesium alloy and steel

Interfaces of immiscible systems are encountered in many situations, such as in layered structures, composites, welds and castings [1–3]. Immiscibility results in an atomically or compositionally sharp interface (no intermixing or transition layer) and weak bonding occurs when the lattice mismatching of the two immiscible elements/compounds is large [4]. In this case, if a transition layer is placed at the interface which is coherent or semicoherent with both sides, the interfacial energy of the immiscible phases can be reduced and a much better bond formed. The objective of this paper is to examine bonding of two immiscible metallic systems by a transition layer which is structurally matched well with both sides.

Mg and Fe were studied as a model because Mg–Fe is a typical immiscible couple which has extremely low (<0.00041 at.%) mutual solid solubility and no compounds form on the Mg–Fe phase diagram [5]. Crystallographic analysis has shown that the lattice mismatch of Fe and Mg is very large [6]. Most recently, it has been found that the Mg/Fe layered structure is a potential magnetoelectronic [7] and hydrogen storage structure [1]. Moreover, Mg/Fe interfaces may also occur in welding (dissimilar welding of Mg to steel) [2] and casting (Fe particles induce heterogeneous solidification of Mg alloy) [8]. Wang et al. found that a nanoscale Fe_2Al_5 layer epitaxially nucleated on Fe substrate during a hot-dipping galvanizing process and the Fe_2Al_5/Fe interface has a low energy with good match of lattice sites [9]. If Fe_2Al_5 can match well with Mg, this nano-Fe_2Al_5 layer could be a transition layer to bond Fe to Mg.

The lattice matching between Fe_2Al_5 and Mg was analyzed first in this study in order to demonstrate that in theory Fe_2Al_5 could be a potential transition layer between Mg and Fe. Based on the lattice parameters $a = 0.7649$ nm, $b = 0.6413$ nm and $c = 0.4217$ nm for orthorhombic Fe_2Al_5 and $a = 0.3209$ nm and $c = 0.5211$ nm for hexagonal close-packed Mg, the possible matching planes and matching directions of Fe_2Al_5 and Mg are shown in Table 1. The interplanar and interatomic misfits for this system are calculated by:

$$\delta = \frac{|\Delta a_0|}{a_0},$$

where Δa_0 is the difference between the interplanar or interatomic distances of the two phases, and a_0 is the respective interplanar or interatomic distances of Fe_2Al_5. In the $\langle 2\bar{1}\bar{1}0\rangle_{Mg}$ // $\langle 0\bar{1}0\rangle_{Fe_2Al_5}$ and $\langle 2\bar{1}\bar{1}0\rangle_{Mg}$ // $\langle 1\bar{1}2\rangle_{Fe_2Al_5}$ directions, the interface between Fe_2Al_5 and Mg is semicoherent [10]. The interplanar mismatching of $\{0002\}_{Mg}$ // $\{021\}_{Fe_2Al_5}$ and $\{01\bar{1}\bar{2}\}_{Mg}$ //

* Corresponding author at: State Key Laboratory of Advanced Welding Production Technology, Harbin Institute of Technology, Harbin 150001, People's Republic of China. Tel./fax: +86 451 86418146; e-mail: ray.plasma@gmail.com

1359-6462/$ - see front matter © 2011 Acta Materialia Inc. Published by Elsevier Ltd. All rights reserved.
doi:10.1016/j.scriptamat.2011.08.026

Table 1. Possible matching planes and directions of Fe_2Al_5 and Mg.

Matching planes or directions	$\{0002\}_{Mg}$ // $\{021\}_{Fe_2Al_5}$	$\{01\bar{1}\bar{2}\}_{Mg}$ // $\{002\}_{Fe_2Al_5}$	$\langle 4\bar{2}\bar{2}0\rangle_{Mg}$ // $\langle 0\bar{1}0\rangle_{Fe_2Al5}$	$\langle 4\bar{2}\bar{2}0\rangle_{Mg}$ // $\langle 1\bar{1}2\rangle_{Fe_2Al_5}$
d-Spacing (mm)				
Mg	0.261	0.190	0.642	0.642
Fe_2Al_5	0.255	0.211	0.642	0.654
Mismatch (%)	2.0	9.8	0	1.8

$\{002\}_{Fe_2Al_5}$ is also small. This crystallographic matching suggests that Fe_2Al_5 can be a suitable solution for use as a potential transition layer to bond immiscible Mg and Fe.

A galvanized steel, which was stated by the supplier to have a Fe_2Al_5 layer between the Zn coating and the steel, was used in this study. In order to confirm the presence of the Fe_2Al_5, the free Zn and Zn–Fe compound layers of the as-received steel were removed using fuming nitric acid (HNO_3), which would leave the Al–Fe layer on the surface if it existed [9,11]. The etched surface was analyzed by energy-dispersive spectrometry (EDS) and X-ray diffraction (XRD). The EDS analysis showed that the surface contained approximately an average of 20 at.% Al and 80 at.% Fe. This result confirmed that Zn was totally removed from the surface of the steel and the layer was Al–Fe intermetallic compound (IMC). Because this IMC layer was extremely thin (of the order of hundreds of nanometers) [9] and the EDS X-rays were generated in a region a few micrometers in depth, the percentage of Al determined by EDS was actually lower than that of the Al–Fe IMC. XRD analysis of the etched steel surface was performed in order to identify the IMC phase, as shown in Figure 1. The Al–Fe IMC layer was identified as Fe_2Al_5: five peaks, including the first three strongest peaks of Fe_2Al_5, i.e. (020), (221) and (002), were well matched. This confirmed that Fe_2Al_5 phase existed between the Zn coating and steel. The two other peaks, around 21.5° and 71.5°, are similar in intensity to the identified Fe_2Al_5 peaks. The peak around 71.5° was noise as confirmed by the XRD raw data. No metallic phases were found to match well with the peak at around 21.5°. It is hard to identify this single peak, but it is believed that it does not affect the existence of Fe_2Al_5 phase.

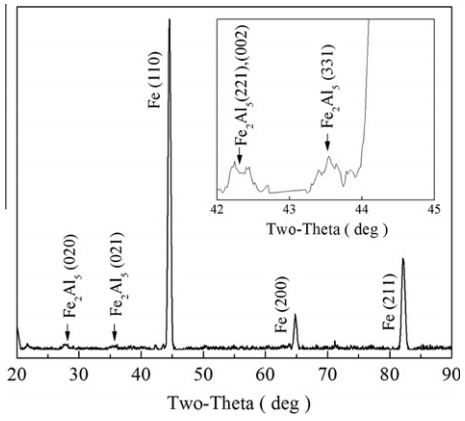

Figure 1. X-ray results of Zn-coated steel surface after etching by fuming HNO_3.

The Zn-coated steel and AZ31 Mg alloy were welded using a medium-frequency DC resistance spot-welding machine. For the purpose of comparison, bare steel (Zn and Fe_2Al_5 mechanically removed) was also welded to AZ31 Mg alloy using the same welding parameters. Details of the welding process have been provided in our previous report [2]. A transmission electron microscopy (TEM) foil of the solid-state joined region (no melting of Mg was observed by scanning electron microscopy) was prepared using the focused ion beam technique according to an in situ lift-out method. Once the TEM foil had been attached to the grid, final thinning was performed on the lamella, initially at an acceleration voltage of 30 kV, and finally at a low voltage of 1 kV since the milling of the Mg matrix is much faster than that of steel. Details of the ion-milling procedure can be found in Ref. [12].

Table 2 compares the mechanical strength of Mg/steel dissimilar joints made with and without the Fe_2Al_5 layer on the steel surface. It can be seen that without a Fe_2Al_5 layer, Mg and steel cannot be joined and the joint strength was almost 0 kN. With the Fe_2Al_5 layer, the joint strength was 4.8 kN, which is comparable to the strength of a Mg/Mg joint [13].

Figure 2 shows the interface of the Mg/steel joint observed by TEM. A continuous nano-interlayer (100–200 nm thick) was found, as shown in Figure 2a. The EDS line scanning indicated that the interlayer was composed of Al and Fe, as shown in Figure 2b. The selected-area electron diffraction pattern (SADP) of the nano-interlayer (top-left in Fig. 2a) identified it as Fe_2Al_5. Since no melting of Mg was found in this region, the peak temperature during joining was below the liquidus of AZ31 Mg alloy (~660 °C). The melting temperature of Fe_2Al_5 is 1169 °C. Hence the Fe_2Al_5 coating did not melt during joining.

The orientation relationships (ORs) of the Fe_2Al_5/Fe and Fe_2Al_5/Mg heterophase interfaces were sequentially determined by a series of SADP and high-resolution TEM (HRTEM) examinations. The SADPs in Figure 3a were taken in the same direction and without tilting, along the zone axis of $[\bar{1}13]_{Fe}$ and $[110]_{Fe_2Al_5}$. The diffraction spot of (002) of Fe_2Al_5 was found to be superimposed with that of (110) of Fe as shown in Figure 3a. This indicated that the crystallographic plane relationship between the Fe and Fe_2Al_5 was $(002)_{Fe_2Al_5}$ // $(110)_{Fe}$. No overlapping diffraction spot from the

Table 2. Tensile shear load of Mg/steel dissimilar joints.

Surface	With Fe_2Al_5	Without Fe_2Al_5 (bare steel)
Load (kN)	4.8	0

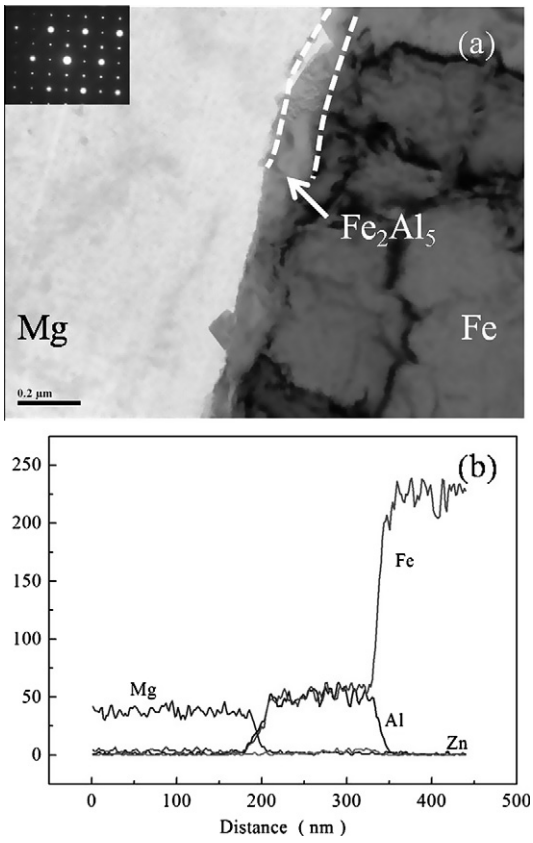

Figure 2. TEM observation and diffraction pattern of the Mg/steel welded interface: (a) interface of bonded Mg and Fe with a Mg/Fe_2Al_5/Fe structure; (b) EDS line scanning of the Mg/Fe interface.

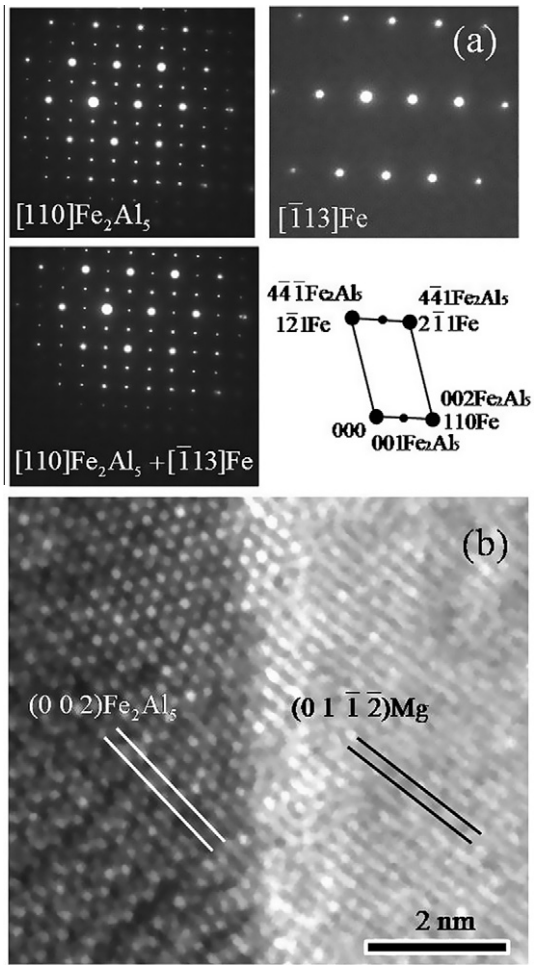

Figure 3. Orientation relationships of the Fe_2Al_5/Fe and Fe_2Al_5/Mg interfaces: (a) diffraction patterns, incident beam parallel to $[1\,1\,0]_{Fe_2Al_5}$ and $[\bar{1}\,1\,3]_{Fe}$; (b) HRTEM of Fe_2Al_5 and Mg.

Fe_2Al_5/Mg interface was observed. However, under HRTEM it was found that the OR of Fe_2Al_5 and Mg was $(002)_{Fe_2Al_5}$ // $(01\bar{1}\bar{2})_{Mg}$ (Fig. 3b). As shown in Table 1, the calculated interplanar distances of $(002)_{Fe_2Al_5}$ and $(01\bar{1}\bar{2})_{Mg}$ were 0.211 and 0.190 nm, respectively. The measured values were 0.21 nm for both $(110)_{Fe}$ and $(002)_{Fe_2Al_5}$, and 0.20 nm for $(01\bar{1}\bar{2})_{Mg}$. The observed interplanar mismatching of Fe_2Al_5/Fe and Fe_2Al_5/Mg heterophase interfaces were 0% and 4.8%, respectively.

According to the edge-to-edge matching model, the matching directions and matching planes are normally the close-packed or nearly close-packed directions and planes [6]. The $(110)_{Fe}$, $(002)_{Fe_2Al_5}$ and $(01\bar{1}\bar{2})_{Mg}$ planes are low-index planes and among the possible or nearly close-packed planes of those phases. Figure 4a–c shows the atomic arrangement of the $(110)_{Fe}$, $(002)_{Fe_2Al_5}$ and $(01\bar{1}\bar{2})_{Mg}$ planes, respectively. For the Fe_2Al_5/Fe interface, the diffraction patterns show that $[\bar{1}13]_{Fe}$ // $[110]_{Fe_2Al_5}$. By overlapping Figure 4a and b with $[\bar{1}13]_{Fe}$ // $[110]_{Fe_2Al_5}$, it can be seen that a semicoherent interface exists in the $[1\bar{1}1]_{Fe}$ and $[1\bar{1}0]_{Fe_2Al_5}$ directions, as shown in Figure 4d). The calculated misfit of $[\bar{1}13]_{Fe}$ and $[110]_{Fe_2Al_5}$ is 5%. Disregarding the small misfit, the overall interface corresponds nearly to a Σ4 boundary and can be a low-energy interface [9]. In short, the Fe_2Al_5 and Fe matched well with the OR $[1\bar{1}0]_{Fe_2Al_5}$ // $[1\bar{1}1]_{Fe}$ and $(002)_{Fe_2Al_5}$ // $(110)_{Fe}$.

According to the zigzag atom-matching model [14], if the distance of an atom to a plane is less than the atomic radius, that atom can be considered as one of the atoms in that plane. Figure 4c shows the atomic arrangement of the $(01\bar{1}\bar{2})_{Mg}$ plane, in which the black spots are atoms of $(01\bar{1}\bar{2})_{Mg}$ and the grey spots are those at a distance of 0.063 nm from the $(01\bar{1}\bar{2})_{Mg}$ plane (the atomic radius of Mg is 0.16 nm). The $[0\bar{1}0]_{Fe_2Al_5}$ and $[100]_{Mg}$ (or $[2\bar{1}\bar{1}0]_{Mg}$) directions are the closest or near closest packed directions in the planes. The atomic distances of the two directions are 0.642 and 0.321 nm, respectively. By overlapping Figure 4b and c, a semicoherent interface can be observed in the $[0\bar{1}0]_{Fe_2Al_5}$ and $[100]_{Mg}$ directions, as shown in Figure 4e. Therefore, the Fe_2Al_5 and Mg can match well with the OR of $[0\bar{1}0]_{Fe_2Al_5}$ // $[100]_{Mg}$ and $(002)_{Fe_2Al_5}$ // $(01\bar{1}\bar{2})_{Mg}$.

These findings can also help us to better understand the grain refinement effect of Fe on Al-containing Mg alloys. Cao et al. [8] have reported that adding Fe to casting pools of Mg alloys AZ31 (3 wt.% Al) and AZ91 (9 wt.% Al) casting pools can refine the grain size to half its former size [8]. Cao et al.'s experimental results further showed that particles present in the central regions of the equiaxed Mg grains were simultaneously Al and Fe rich. Since crystallographic matching between nuclei and matrix is critical for heterogeneous nucleation, the lattice-matching analysis in this study suggests that

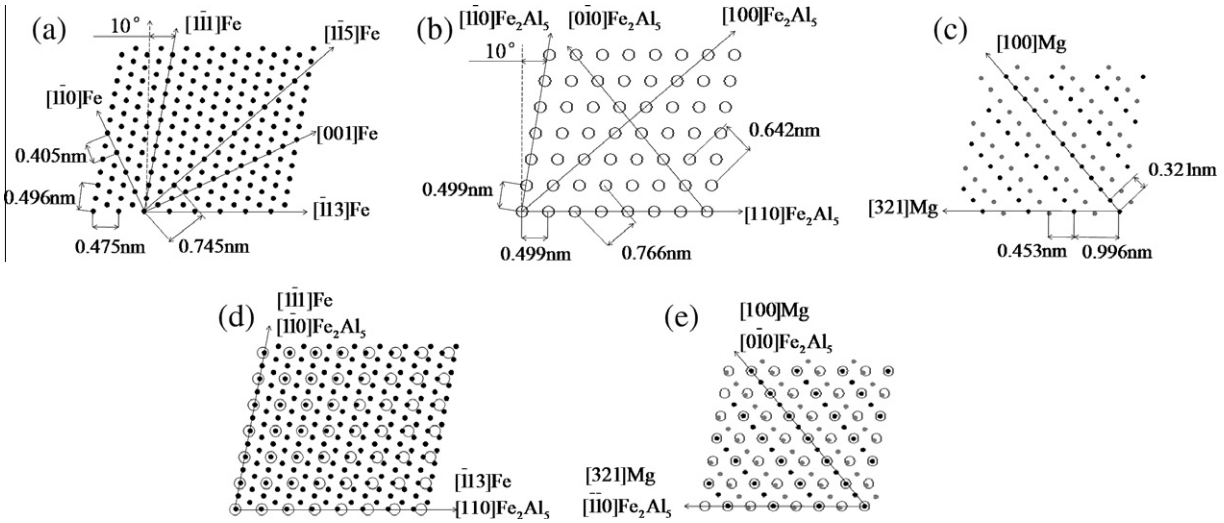

Figure 4. Atomic arrangement of $(110)_{Fe}$, $(002)_{Fe_2Al_5}$ and $(01\bar{1}\bar{2})_{Mg}$: (a) $(110)_{Fe}$; (b) $(002)_{Fe_2Al_5}$; (c) $(01\bar{1}\bar{2})_{Mg}$; (d) $(110)_{Fe}$ and $(002)_{Fe_2Al_5}$; (e) $(002)_{Fe_2Al_5}$ and $(01\bar{1}\bar{2})_{Mg}$.

those Al–Fe particles may be Fe_2Al_5 which led to heterogeneous nucleation during solidification and refined the grain size.

In summary, immiscible Mg and Fe were successfully bonded via a nanoscaled Fe_2Al_5 transition layer that had been coated onto the Fe surface. As-expected, low-energy interfaces with well-matching lattice sites were observed. The ORs of the Fe_2Al_5/Fe heterophase interface were $[1\bar{1}0]_{Fe_2Al_5}$ // $[1\bar{1}1]_{Fe}$ and $(002)_{Fe_2Al_5}$ // $(110)_{Fe}$. The ORs of the Fe_2Al_5/Mg heterophase interface were $[0\bar{1}0]_{Fe_2Al_5}$ // $[100]_{Mg}$ and $(002)_{Fe_2Al_5}$ // $(01\bar{1}\bar{2})_{Mg}$. The finding of a well-matched Fe_2Al_5/Mg heterophase interface can also explain the heterogeneous nucleation of α-Mg during solidification of Al-containing Mg alloys with added Fe.

This research is financially supported by the Natural Sciences and Engineering Research Council (NSERC) of Canada in the Framework of Strategic Magnesium Network Program (MagNet) and AUTO21 Network of Centres of Excellence of Canada. The authors would like to thank Julia Huang and Mr. Fred Pearson from the Canadian Centre for Electron Microscopy, McMaster University, for help with preparing TEM films with FIB and TEM observation. Appreciation is also expressed to Prof. Scott Lawson, Drs. Yuquan Ding and Xiaogang Li from University of Waterloo for useful discussions.

[1] W.P. Kalisvaart, A. Kubis, M. Danaie, B.S. Amirkhiz, D. Mitlin, Acta Mater. 59 (2011) 2083–2095.
[2] L. Liu, L. Xiao, J.C. Feng, Y.H. Tian, S.Q. Zhou, Y. Zhou, Metall. Mater. Trans. A 41 (2010) 2651–2661.
[3] S. Ohsaki, K. Yamazaki, K. Hono, Scripta Mater. 48 (2003) 1569–1574.
[4] Y. Mishin, M. Asta, J. Li, Acta Mater. 58 (2010) 1117–1151.
[5] T. Haitani, Y. Tamura, T. Motegi, N. Kono, H. Tamehiro, Mater. Sci. Forum 419 (2003) 697–702.
[6] M.X. Zhang, P.M. Kelly, Acta Mater. 53 (2005) 1073–1084.
[7] Y. Wang, J. Zhang, X.G. Zhang, H.P. Cheng, X.F. Han, Phys. Rev. B 82 (2010) 054405.
[8] P. Cao, M. Qian, D.H. St. John, Scripta Mater. 51 (2004) 125–129.
[9] K.K. Wang, L. Chang, D. Gan, H.P. Wang, Thin Solid Films 518 (2010) 1935–1942.
[10] R. Benedek, D.N. Seidman, C. Woodward, J. Phys.: Condens. Matter 14 (2002) 2877–2900.
[11] E. McDevitt, Y. Morimoto, M. Meshii, ISIJ Int. 37 (1997) 776–782.
[12] L. Zaykova-Feldman, T.M. Moore, Microsc. Microanal. 11 (2005) 848–849.
[13] S. Zhou, L. Liu, J.P. Jung, M.Y. Lee, Y.N. Zhou, Met. Mater. Int. 16 (2010) 967–974.
[14] M.X. Zhang, P.M. Kelly, M. Qian, J.A. Taylor, Acta Mater. 53 (2005) 3261–3270.